International Journal of Microwave and Wireless Technologies, 2017, 9(5), 1059–1065.
doi:10.1017/S175907871600129X

RESEARCH PAPER

Waveguide T-junctions with resonant coupling between sections of different dimensions

SERGEY L. BERDNIK, VICTOR A. KATRICH, MIKHAIL V. NESTERENKO AND YURIY M. PENKIN

Electromagnetic characteristics of the E-plane T-junction for two rectangular waveguides using resonant coupling between the waveguide sections were studied by mathematical modeling. The problem of coupling between infinite and semi-infinite rectangular waveguides through a resonant slot in the end-wall of the semi-infinite waveguide in the presence of resonant monopole is solved in a strict electrodynamic formulation. The monopole with variable surface impedance is placed parallel to the narrow walls at an arbitrary position inside the infinite waveguide. The problem is solved analytically by the generalized method of induced electro-magneto-motive forces. Impedance vibrator inclusions with variable electro-physical parameters have been analyzed as control elements for waveguide junctions. To this purpose energy characteristics of the junction in the single-mode regime of the both waveguides, and also in multi-mode regime of the semi-infinite waveguide is investigated. The results may be useful for development of variety antennas and waveguide devices, which involves waveguide junctions.

Keywords: Modeling, Simulation and characterizations of devices and circuits, Passive components and circuits

Received 16 May 2016; Revised 17 October 2016; Accepted 20 October 2016; first published online 23 November 2016

I. INTRODUCTION

Waveguide *E*- and *H*- plane junctions are widely used in modern antenna-feeder equipments working at microwave and extremely high frequencies [1–5]. Junction matching is usually carried out by inductive or capacitive diaphragms [6, 7], and resonant metal rods [7, 8] in the straight waveguide. The rods are preferable, since they do not block the waveguide cross-section. In almost all publications on this topic, the rods were assumed to be perfectly conducting and located in the coupling area symmetrically with respect to the waveguide walls. In this paper, the first in literature, we consider the resonant coupling problem between an infinite rectangular waveguide, in which is located parallel to the narrow walls monopole with variable along their axis surface impedance, and a semi-infinite waveguide through a resonant slot in its end-wall. Also feature of the proposed junction design is monopole-slot coupling between the two waveguides of different cross-sections. Mathematical modeling plays an important role in the development of complex waveguide devices, since their experimental optimization is extremely time consuming, expensive, and sometimes impossible.

V. N. Karazin Kharkiv National University, 4, Svobody Sq., Kharkiv 61022, Ukraine.
Phone: +38 057 707 5585
Corresponding author:
M.V. Nesterenko
Email: mikhail.v.nesterenko@gmail.com

However, we must understand that a direct numerical analysis of the junction with any commercial software, such as Ansoft HFSS (high frequency structural simulator), is a complex and quite tedious problem. First, the analysis must be performed using an integrated approach, which should combine various software tools for computing characteristic of separate device fragments. Second, 3D rendering of the vibrator scatterer with variable surface impedance is a complicated problem. This is related to the fact that physical implementation of the vibrator with a predefined impedance distribution over its surface is a separate problem of design synthesis. Third, the usage of several discrete ports in coupling area of the slot that is necessary for multimode excitation of side waveguides requires a step-by-step design algorithm and additional analysis of its physical adequacy. Thus, the modeling of the waveguide junction using Ansoft HFSS package can be associated with both unreasonable costs of computer resources and long development time, so that it may become ineffective as compared with the proposed method based on the numerical and analytical solution of boundary value problem.

This paper is aimed at creating a mathematical model of the T-junction. The model is applied to study energy characteristics of the junction in the single-mode regime of both waveguides and to explore multi-mode excitation of the side semi-infinite waveguide, since this type of excitation is not yet sufficiently covered in the literature [8]. The electromagnetic problem of fundamental mode scattering in the straight waveguide is formulated and analytically solved by the well-proven generalized

method of induced electro -magneto-motive forces (EMMF) [9–12] in Section II. The energy characteristics of the junction obtained by modeling are presented in Section III. The overall results and some practical advice concerning designing the T-junctions are given in the Conclusion.

II. FORMULATION OF THE PROBLEM AND SOLUTION OF INTEGRAL EQUATIONS FOR THE CURRENTS

Let the fundamental wave TE_{10} propagates in a hollow infinite rectangular waveguide with perfectly conducting walls (the area index is "Wg1") from the region $z = -\infty$. In the plane of the waveguide cross-section, a thin asymmetrical vibrator (monopole) with variable surface impedance, contacting with the waveguide wall, is placed parallel to the narrow waveguide walls. The waveguide dimension is $\{a \times b\}$, the monopole radius is r and its length is L_v ($(r_v/L_v) \ll 1$, $(r/\lambda) \ll 1$, λ is wavelength in free space). A narrow transverse slot in the waveguide broad wall radiates into the hollow semi-infinite rectangular waveguide with cross section $\{a_2 \times b_2\}$ (the area index is "Wg2"). The slot is cut symmetrically relative to the line $y_2 = b_2/2$; the thickness, width and length of the slot are h, d, and $2L_{sl}$ ($[d/(2L_{sl})] \ll 1$, $(d/\lambda) \ll 1$), respectively. Further we will use only one boundary condition for the magnetic field in the slot aperture, and take into account the wall thickness h of the waveguide section in which the slot is cut [10]. Displacement of the monopole in the cross section relative to the waveguide narrow wall is x_0. The slot center is shifted at a distance x_{01} relative to the narrow wall of the straight waveguide, and the slot center in the end-wall of the side waveguide is shifted at x_{02}. The distance between the monopole and slot axes is equal to z_0 (Fig. 1).

If time dependence is $e^{i\omega t}$ (ω is the circular frequency, t is time) the initial system of integral equations for the electric current on the monopole $J_v(s_1)$ and the equivalent magnetic current in the slot $J_{sl}(s_2)$, which in the framework of accepted approximations for electrically thin radiators are one-dimensional, can be written as [9]

$$\left(\frac{d^2}{ds_1^2}+k^2\right)\int_{-L_v}^{L_v} J_v(s_1')G_{s_1}^{Wg1}(s_1,s_1')ds_1' - ik\int_{-L_{sl}}^{L_{sl}} J_{sl}(s_2')\tilde{G}_{s_2}^{Wg1}(s_1,s_2')ds_2' = -i\omega\left[E_{os_1}(s_1)-z_i(s_1)J_v(s_1)\right], \tag{1a}$$

$$\left(\frac{d^2}{ds_2^2}+k^2\right)\int_{-L_{sl}}^{L_{sl}} J_{sl}(s_2')\left[G_{s_2}^{Wg1}(s_2,s_2')+G_{s_2}^{Wg2}(s_2,s_2')\right]ds_2' - ik\int_{-L_v}^{L_v} J_v(s_1')\tilde{G}_{s_1}^{Wg1}(s_2,s_1')ds_1' = -i\omega H_{os_2}(s_2). \tag{1b}$$

Here s_1 and s_2 are local coordinates along the monopole and slot axes, respectively; $z_i(s_1)$ (Ω/m) is internal linear impedance of the monopole; $E_{os_1}(s_1)$ and $H_{os_2}(s_2)$ are projections of the components of the H_{10}-wave field onto the monopole and slot axes, respectively; $G_{s_1}^{Wg1}(s_1,s_1')$ and $G_{s_2}^{Wg1,2}(s_2,s_2')$ are the Green's functions components of electric and magnetic type for the infinite and semi-infinite waveguides [10, 11]; "$-L_v$" is the coordinate of mirror image of the monopole end relative to the bottom broad wall of the straight waveguide [11]; $J_v(\pm L_v)=0$, $J_{sl}(\pm L_{sl})=0$; $\tilde{G}_{s_1}^{Wg1}(s_2,s_1')=(\partial/\partial z)G_{s_1}^{Wg1}[x(s_2),0,z;x'(s_1'),y'(s_1'),z_0]$, $\tilde{G}_{s_2}^{Wg1}(s_1,s_2')=(\partial/\partial z)G_{s_2}^{Wg1}[x(s_1),y(s_1),z;x'(s_2'),0,0]$ under condition that $z=0$ and $z=z_0$ are substituted respectively into $\tilde{G}_{s_1}^{Wg1}$ and $\tilde{G}_{s_2}^{Wg1}$ after derivation; $k=2\pi/\lambda$.

We will seek the solution of the equations system (1) by a generalized method of induced EMMF [9–11], using functions $J_v(s_1)=J_{ov}\,f_v(s_1)$ and $J_{sl}(s_2)=J_{osl}\,f_{sl}(s_2)$ as approximating expressions for the currents. Here J_{ov} and J_{osl} are unknown current amplitudes, $f_v(s_1)$ and $f_{sl}(s_2)$ are predetermined functions of the current distributions, which can be derived as the solution of equation (1) by the asymptotic averaging method for the solitary monopole and solitary slot under condition $z_0=0$ [10, 11]. For our monopole-slot structure excited by the H_{10} wave we have

$$f_v(s_1)=\cos\tilde{k}s_1-\cos\tilde{k}L_v, \tag{2a}$$

$$f_{sl}(s_2)=\cos ks_2-\cos kL_{sl}, \tag{2b}$$

where $\tilde{k}=k-i2\pi z_i^{av}/(Z_0\Omega)$, $z_i^{av}=1/(2L_v)\int_{-L_v}^{L_v} z_i(s_1)ds_1$ is the average value of the internal impedance along the monopole length [11], $Z_0=120\pi\,\Omega$, $\Omega=2\ln(2L_v/r)$. Then we multiply the equations (1a) and (1b) by the functions $f_v(s_1)$ and $f_{sl}(s_2)$, respectively, and integrate the equation (1a) along the length of the monopole and equation (1b) along the length of the slot. Thus, we obtain a system of linear algebraic equations whose solution is the currents amplitudes J_{ov}, J_{osl}

$$\begin{aligned} J_{ov}(Z_{11}+F_z)+J_{osl}Z_{12}&=-i\omega/(2k)E_1,\\ J_{osl}(Z_{22}^{Wg1}+Z_{22}^{Wg2})+J_{ov}Z_{21}&=-i\omega/(2k)H_2. \end{aligned} \tag{3}$$

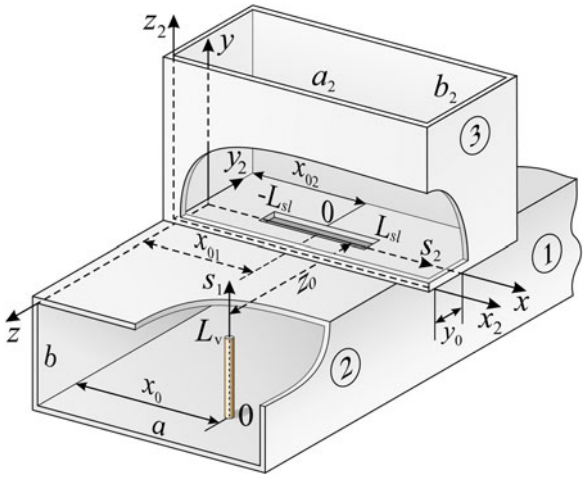

Fig. 1. The geometry of structure and notations.

Here

$$Z_{11} = \frac{4\pi}{ab}\sum_{m=1}^{\infty}\sum_{n=0}^{\infty}\left[\frac{\varepsilon_n(k^2-k_y^2)\tilde{k}^2}{kk_z(\tilde{k}^2-k_y^2)^2}e^{-k_z r}\right.$$
$$\left.\sin^2 k_x x_0\left[\sin\tilde{k}L_v\cos k_y L_v - (\tilde{k}/k_y)\cos\tilde{k}L_v\sin k_y L_v\right]^2\right],$$

$$Z_{12} = Z_{21} = \frac{4\pi}{ab}\sum_{m=1}^{\infty}\sum_{n=0}^{\infty}\left[\frac{\varepsilon_n k\tilde{k}e^{-k_z z_0}}{i(k^2-k_x^2)(\tilde{k}^2-k_y^2)}\sin k_x x_0\sin k_x x_{01}\right.$$
$$\times\left[\sin\tilde{k}L_v\cos k_y L_v - (\tilde{k}/k_y)\cos\tilde{k}L_v\sin k_y L_v\right]$$
$$\left.\times\left[\sin kL_{sl}\cos k_x L_{sl} - (k/k_x)\cos kL_{sl}\sin k_x L_{sl}\right]\right],$$

$$Z_{22}^{Wg1} = \frac{8\pi}{ab}\sum_{m=1}^{\infty}\sum_{n=0}^{\infty}\left[\frac{\varepsilon_n k e^{-k_z(d_e/4)}}{k_z(k^2-k_x^2)}\sin^2 k_x x_{01}\right.$$
$$\left.[\sin kL_{sl}\cos k_x L_{sl} - (k/k_x)\cos kL_{sl}\sin k_x L_{sl}]^2\right],$$

$$Z_{22}^{Wg2} = \frac{16\pi}{ab}\sum_{m=1}^{\infty}\sum_{n=0}^{\infty}\left[\frac{\varepsilon_n k}{k_z(k^2-k_x^2)}\sin^2 k_x x_{02}\cos k_y y_0\cos k_y\right.$$
$$\left.\left(y_0+\frac{d_e}{4}\right)[\sin kL_{sl}\cos k_x L_{sl} - (k/k_x)\cos kL_{sl}\sin k_x L_{sl}]^2\right],$$
$$Z_{22}^{\Sigma} = Z_{22}^{Wg1} + Z_{22}^{Wg2}; \tag{4}$$

$$E_1 = 2H_0\left[k/(k_g\tilde{k})\right]\sin(\pi x_0/a)e^{-ik_g z_0}f(\tilde{k}L_v),$$
$$f(\tilde{k}L_v) = \sin\tilde{k}L_v - \tilde{k}L_v\cos\tilde{k}L_v,$$
$$H_2 = 2H_0(1/k)\sin(\pi x_{01}/a)f(kL_{sl}),$$
$$f(kL_{sl}) = \frac{\sin kL_{sl}\cos(\pi L_{sl}/a) - (ka/\pi)\cos kL_{sl}\sin(\pi L_{sl}/a)}{1-[\pi/(ka)]^2},$$
$$F_z = -\frac{i}{r}\int_0^{L_v} f_v^2(s_1)\bar{Z}_{SV}(s_1)\mathrm{d}s_1. \tag{5}$$

In the formulas (4) and (5) $\varepsilon_n = \begin{cases}1, & n=0\\ 2, & n\neq 0\end{cases}$, $k_x = m\pi/a(a_2)$, $k_y = n\pi/b(b_2)$, $k_z = \sqrt{k_x^2+k_y^2-k^2}$, $k_g = \sqrt{k^2-(\pi/a)^2}$, m and n are integers; $\bar{Z}_S(s_1) = \bar{R}_S + i\bar{X}_S\phi(s_1)$ is the distributed surface impedance normalized to Z_0 $\bar{Z}_S(s_1) = 2\pi r z_i(s_1)$, $\phi(s_1)$ is the given function, $d_e = d\exp(-\pi h/2d)$ is equivalent slot width [9], which take into account the actual wall thickness h of the waveguide.

Solution of the equation system (3) can be written as

$$J_{ov} = -\frac{i\omega}{2k}\frac{E_1 Z_{22}^{\Sigma} - H_2 Z_{12}}{(Z_{11}+F_z)Z_{22}^{\Sigma} - Z_{21}Z_{12}} = -\frac{i\omega H_0}{k^2}J_v,$$
$$J_{osl} = -\frac{i\omega}{2k}\frac{H_2(Z_{11}+F_z) - E_1 Z_{21}}{(Z_{11}+F_z)Z_{22}^{\Sigma} - Z_{21}Z_{12}} = -\frac{i\omega H_0}{k^2}J_{sl}. \tag{6}$$

The currents on the monopole and in the slot can be obtained using (2) and (6)

$$J_v(s_1) = -H_0(i\omega/k^2)J_v(\cos\tilde{k}s_1 - \cos\tilde{k}L_v),$$
$$J_{sl}(s_2) = -H_0(i\omega/k^2)J_{sl}(\cos ks_2 - \cos kL_{sl}), \tag{7}$$

where H_0 is the amplitude of TE_{10} wave. The reflection and transmission coefficients, S_{11} and S_{21} in the straight waveguide can be represented as

$$S_{11} = \frac{4\pi i}{abk}\left\{\frac{2k_g}{k}J_{sl}\sin\frac{\pi x_{01}}{a}f(kL_{sl})\right.$$
$$\left.-\frac{k}{\tilde{k}}J_v\sin\frac{\pi x_0}{a}e^{-ik_g z_0}f(\tilde{k}L_v)\right\}e^{2ik_g z}, \tag{8}$$

$$S_{21} = 1 + \frac{4\pi i}{abk}\left\{\frac{2k_g}{k}J_{sl}\sin\frac{\pi x_{01}}{a}f(kL_{sl})\right.$$
$$\left.+\frac{k}{\tilde{k}}J_v\sin\frac{\pi x_0}{a}e^{ik_g z_0}f(\tilde{k}L_v)\right\}. \tag{9}$$

The number of propagating wave modes M in the side waveguide section Wg2 depends upon the dimensions of the waveguide cross section $\{a_2\times b_2\}$. Therefore, the scattering matrix of the waveguide junction contains the power reflection and transmission coefficient $P_{11} = |S_{11}|^2$, $P_{21} = |S_{21}|^2$ for the propagating mode in the straight waveguide and a number of power transmission coefficients P_{31}^{mn} for the propagating modes in the side waveguide. The coefficients P_{31}^{mn} are determined by the formula $P_{31}^{mn} = P_{31}(P_{sl}^{mn}/P_{\Sigma sl}^{mn})$, where $P_{31} = 1 - P_{11} - P_{21} - P_{\sigma v}$, $(P_{sl}^{mn}/P_{\Sigma sl}^{mn})$ is the power ratio of the partial waves to the total power of waves propagating in the arm Wg2, normalized to the power of the wave TE_{10} coming from the generator, $P_{\sigma v}$ is the power loss in the monopole, which can be determined using the energy balance equation $P_{11v} + P_{21v} + P_{\sigma v} = 1$ for the auxiliary problem with the slot metallization. For asymmetric waveguides junctions (Fig. 1) under conditions $y_0 = b_2/2$, the expression for the magnetic type wave propagating in the side waveguide arm can be presented as

$$P_{sl}^{mo} = \frac{a_2 b_2 k_g}{abk_g^{mo}}\left|\frac{16\pi k_g^{mo}\sin(\pi x_{01}/a)f(kL_{sl})\sin(m\pi x_{02}/a_2)f_{sl}^{mo}}{a_2 b_2 k^3 Z_{22}^{\Sigma}}\right|^2, \tag{10}$$

where

$$f_{sl}^{mo} = \frac{\sin kL_{sl}\cos(m\pi L_{sl}/a_2) - (ka_2/m\pi)\cos kL_{sl}\sin(m\pi L_{sl}/a_2)}{1-[m\pi/(ka_2)]^2},$$

$$k_g^{mo} = \sqrt{k^2-(m\pi/a)^2}$$

and

$$P_{\Sigma sl}^{mo} = \sum_{m=1}^{M} P_{sl}^{mo}.$$

It is known [11] that the impedance vibrators can be tuned to resonance if its length is less than that of the perfectly conducting vibrators and the surface impedance of the inductive type ($\bar{X}_S > 0$) is used. If a junction works at large power, the electrical breakdown can occur between the monopole end and waveguide wall. Therefore, it is appropriate to employ

inductive surface impedance. All modeling results presented below were obtained using surface impedance distributed along the monopole axis according to functions: constant ϕ_0 $(s_1) = 1$ and cosine ϕ_1 $(s_1) = (\pi/2)\cos\pi s_1/2L_v$ distribution functions. If the constant distribution function is used, the expression (5) has the form

$$F_z^{\phi_0} = -\frac{iL_v(\bar{R}_S + i\bar{X}_S)}{2r}\left[(2+\cos 2\tilde{k}L_v) - 3\frac{\sin 2\tilde{k}L_v}{2\tilde{k}L_v}\right] = F_z^c(\bar{R}_{SV} + i\bar{X}_{SV})\Phi_z^c. \quad (11)$$

For the cosine function we have

$$F_z^{\phi_1} = F_z^c\left\{\bar{R}_S\Phi_z^c + i\bar{X}_S\left[\frac{\pi^2\cos 2\tilde{k}L_v}{\pi^2 - (4\tilde{k}L_v)^2} - 2\cos\tilde{k}L_v\frac{\pi^2 + (2\tilde{k}L_v)^2}{\pi^2 - (2\tilde{k}L_v)^2} + 1\right]\right\}. \quad (12)$$

Formulas for surface impedances of thin vibrators, obtained by the authors in the framework of the impedance concept are given in [11].

III. NUMERICAL RESULTS

Our mathematical model allows effective computation of the energy characteristics for waveguide junctions both with and without the monopole. The program base on the model is by several orders of magnitude faster than commercial software. The program base on the model is by several orders of magnitude faster than any commercial software. In our approximation, the inequalities $2r_v/L_v \le 1$ and $[d/(2L_{sl})]$ hold, and the numbers of terms in double series (4) was chosen to provide the calculation of the matrix coefficients in each of the coupling areas with an accuracy of 0.1%.

Figure 2 shows the junction energy characteristics versus the wavelength, P_{q1}, $q = 1, 2, 3$, for the solitary slot without the monopole used for coupling between the infinite and semi-infinite single-mode waveguides. All computations were performed using the following geometrical parameters of the structure: $a = 58$, $b = 25$, $d = 4$, $h = 0.5$, $r = 2$ mm, $x_o = a/8$, $y_o = b_2/2$. As can be seen, the powers of waves transmitted into arms 2 and 3 are equal if the slot resonant wavelength is $\lambda_{sl}^{res} \approx 80$ mm amounting up to 90% of the incident wave power. About 10% of the incident power is reflected back to the generator. The slot length is chosen so that its resonant wavelength is in the middle of the operating waveband. The general theory of slot radiators predicts three features of the junction structure: (1) no more than 50% of the incident wave power can be directed into the side waveguide, and the power can be divided in the range $(1/6) \le P_{31}^{10}/P_{21} \le 1$ by selection of the operating wavelength; (2) the power division between the arms in the ratio 1:1 can be achieved only at the slot resonant wavelength when the highest reflection is observed in the straight waveguide; (3) resonant coupling of the waveguides determines the relative band limitedness as

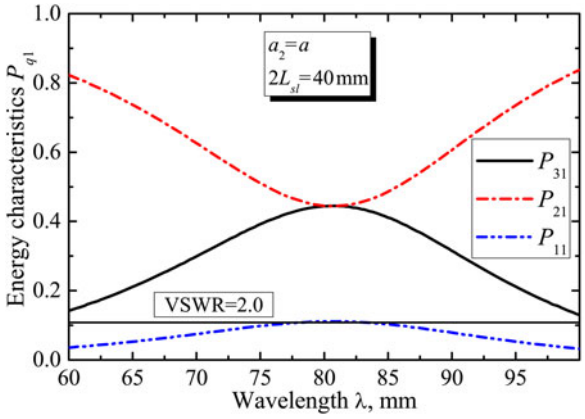

Fig. 2. The energy characteristics versus wavelength for the solitary slot: $b_2 = b$, $x_{o1} = x_{o2} = a/2$.

compared with bridge-type junctions for any mode of power division between the arms. The first two restrictions can be eliminated by introducing the impedance monopole in the straight waveguide near the slot. Indeed, if a monopole with a constant impedance is placed at the distance $z_o = \lambda_G^{Sres}/2$ (here $\lambda_G^{Sres} = 2\pi/\sqrt{(2\pi/\lambda_{sl}^{res})^2 - (\pi/a)^2}$) from the slot longitudinal axis a significant increase in the power of the transmitted wave in the arm 3 (up to 90%) and decrease P_{21} и P_{11} is observed at resonant wavelength of the slot and monopole $\lambda_{sl}^{res} = \lambda_v^{res} \approx 80$ mm (Fig. 3(a), $z_o = 54$ mm). It is also possible to divide power of the transmitted waves in a predetermined ratio at certain wavelengths of operating band (in the range $60 \div 80$ mm) with a sufficiently satisfactory arm matching. Figures 3(b) and 3(c) show the energy characteristics of the monopole, which length is $L_v = 15$ mm. These characteristics coincide with that of the monopole in Fig. 3(a), but have different resonant wavelengths: (b) $\lambda_v^{res} \approx 72$ mm (perfectly conducting monopole), (c) $\lambda_v^{res} \approx 88$ mm (monopole with variable impedance). In these cases, the power of the transmitted waves can be divided in predefined ratio at some wavelengths in the operating waveband $73 \div 100$ mm (see Figs 3(b) and 3(c)) with satisfactory matching in the arm 1 (voltage standing wave ratio, VSWR ~ 2.0).

The revealed physical mechanisms were confirmed by experimental results for the monopole with variable impedance and are shown in Fig. 4, where the picture of experimental monopole model is also shown. The experimental model have been made in the form of corrugated brass rod with the crests thickness 1 mm, the notch width 1 mm, and the inner radius $r_i(s_v) = r\ \exp[-\ln(4.0)\phi_1(s_v)]$. Here, as in other cases of the comparative analysis [9–12], the design characteristics of the slot and vibrator-slot waveguide structures obtained by the generalized EMMF method differ from experimental data by no more than 2–5%. Note that the maximum difference is observed if distances z_o between the vibrator and slot is of order of several slot widths d. This can be explained by scattering of cross-polarization fields on joint elements.

The possibility of transferring most of the incident power from the straight waveguide into the side waveguide can be used to organize additional modal channels of power division in the side waveguide. The regimes of equal power division between the separate modes in the side arm of the waveguide structure and between all the physical channels of the power division are of particular interest for practical applications.

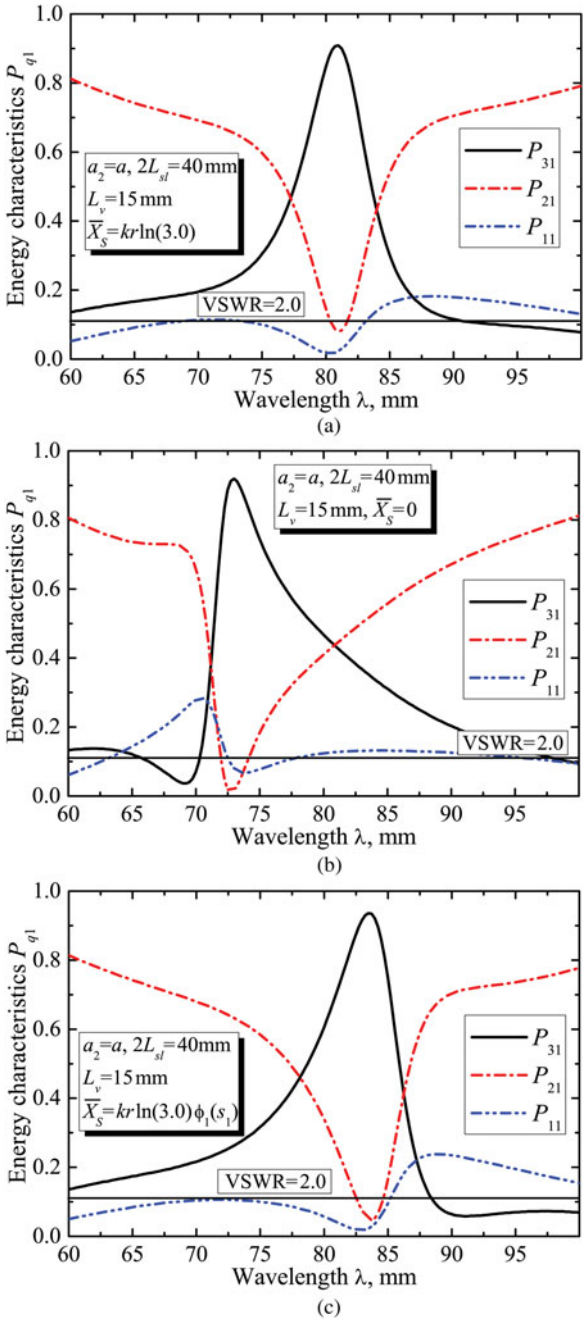

Fig. 3. The energy characteristics versus wavelength for the slot-monopole system: $b_2 = b$, $z_0 = 54$ mm, $x_{01} = x_{02} = a/2$.

Our calculations have shown that such regimes can be realized. Thus, if the size of the side waveguide broad wall is increased 2 times, the TE_{10} and TE_{20} waves are efficiently excited (Fig. 5) while the amplitude of TE_{30} wave is negligibly small. A roughly equal division of power between the transmitted waves TE_{10} and TE_{20} in the wavelength band $\lambda \in [93, 98.5]$ mm can be achieved by varying the monopole surface impedance and slot length. At the wavelength of 95 mm 90% of the incident power is transmitted from the straight waveguide into the side arm at the optimum matching and equal division of power between the excited modes ($P_{31}^{10} = P_{31}^{20} \approx 0.45$). At wavelengths of 92.5 and 97.5 mm the regime of equal division among all the physical channels is observed ($P_{21} = P_{31}^{10} = P_{31}^{20} \approx 0.3$).

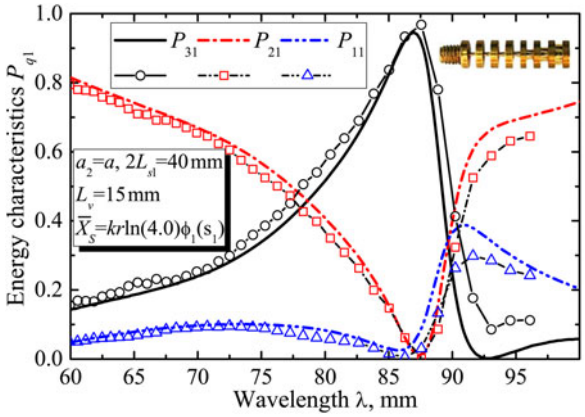

Fig. 4. The energy characteristics versus wavelength for the slot-monopole system: $b_2 = b$, $z_0 = 54$ mm, $x_{01,2} = a/2$, (circles – experimental data).

These trends of the power division are also observed when the waveguide side walls are decreased in order to reduce weight and dimensions of waveguide structures. In this case, it is possible to implement the regime of equal power division at shorter wavelengths. For example, if the side wall of the waveguide is reduced by 50%, the powers P_{31}^{10} and P_{31}^{20} are approximately equal in the waveband $\lambda \in [69, 74]$ and are divided in various ratios with P_{21} (Fig. 6). At the resonant

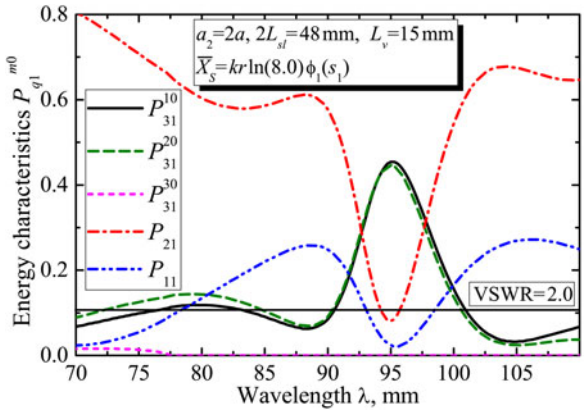

Fig. 5. The energy characteristics versus wavelength for the slot-monopole system: $b_2 = b$, $z_0 = 85$ mm, $x_{01} = a/2$, $x_{02} = a_2/4$.

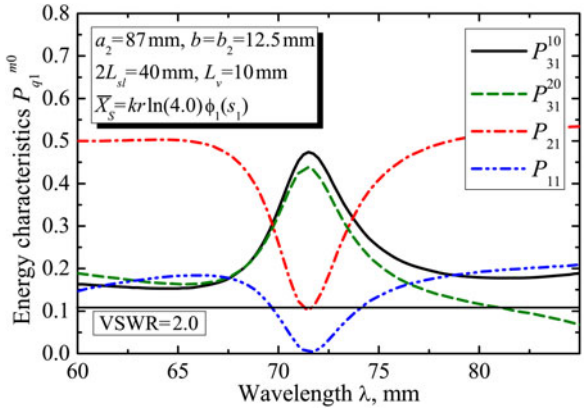

Fig. 6. The energy characteristics versus wavelength for the slot-monopole system: $z_0 = 46$ mm, $x_{01} = a/2$, $x_{02} = a_2/4$.

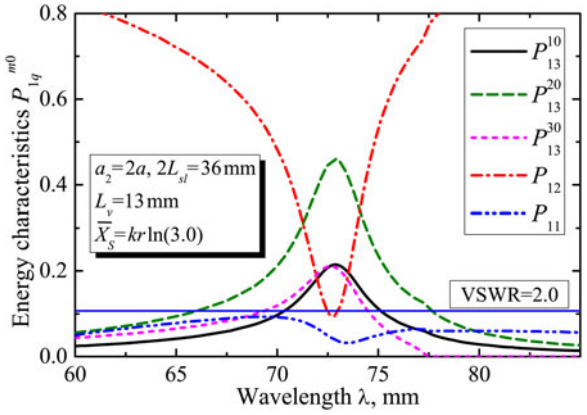

Fig. 7. The energy characteristics versus wavelength for the slot-monopole system: $b_2 = b$, $z_0 = 46$ mm, $x_{01} = a/3$, $x_{02} = a_2/6$.

wavelengths of the monopole and slot, $\lambda_v^{res} = \lambda_{sl}^{res} \approx 71.5$ mm the reflection coefficient in the straight waveguide is almost zero, and 90% of the incident power transmitted into the side waveguide arm is equally divided between propagating modes, $P_{31}^{10} = P_{31}^{20} \approx 0.45$.

If the slot length is reduced and the slot center is shifted to the narrow wall of the straight waveguide at $x_{01} = a/3$, then $x_{02} = a_2/6$, and the slot center is located at the antinode of the TE_{30} wave, the wave TE_{30} along with the waves TE_{10} and TE_{20} will effectively be excited in the side waveguide (Fig. 7). The coefficients P_{31}^{10} and P_{31}^{30} in the middle of the band are almost equal. These coefficients equal to P_{21} at two wavelengths, and the coefficient P_{31}^{20} is almost twice greater than P_{21}. At the resonant frequency, ratio $P_{31}^{20} \approx P_{31}^{10} + P_{31}^{30}$ holds.

IV. CONCLUSION

The energy characteristics of the *E*-plane T-junction for the rectangular waveguides were obtained by the mathematical modeling carried out on the basis of the analytical solution of the internal diffraction problem by the generalized method of induced EMMF. The system consisting of the impedance monopole in the infinite waveguide and the slot in the end-wall of the semi-infinite waveguide section is placed in the coupling area of the junction. The validity of the simulation results and the physical correctness of the approximations used for the problem solution is confirmed experimentally. Also note that the energy parameters of waveguide structures with a single slot and a perfectly conducting vibrator (not represented here graphically) obtained by the generalized method of induced EMMF and by the commercial software Ansoft HFSS are in good agreement.

As opposed to bridge-type junctions, the proposed construction is a resonant narrow-band device. Therefore, the waveguide structures of this type for a long time were not very interesting for the researchers. At present, multi-function devices are widely used in many practical applications, therefore the interest in such structures begins to grow. Particular attention is drawn to junctions functioning in multimode regime of power division, which allows controlling of this process. It has been shown that it is possible to achieve the division of power between the junction coupling arms and modes of propagating waves in a wide range by changing the geometric dimensions of the junction elements, surface impedance, and the distribution function of the surface impedance along the monopole. The present solution of the problem without much difficulty can be extended to multi-element vibrator-slot structures [12].

REFERENCES

[1] Lewin, L.: Theory of Waveguides. Techniques for the Solution of Waveguide Problems, Newnes-Butterworths, London, 1975.

[2] Arndt, F.; Ahrens, I.; Papziner, U.; Wiechmann, U.; Wilkeit, R.: Optimized E-plane T-junction series power dividers. IEEE Trans. Microw. Theory Tech., **35** (1987), 1052–1059.

[3] Yao, H.-W.; Abdelmonem, A.E.; Liang, J.-F.; Liang, X.-P.; Zaki, K.A.; Martin, A.: Wide-band waveguide and ridge waveguide T-junctions for diplexer applications. IEEE Trans. Microw. Theory Tech., **41** (1993), 2166–2173.

[4] Kirilenko, A.A.; Senkevich, S.L.; Tkachenko, V.I.; Tysik, B.G.: Waveguide diplexer and multiplexer design. IEEE Trans. Microw. Theory Tech., **42** (1994), 1393–1396.

[5] Widarta, A.; Kuwano, S.; Kokubun, K.: Simple and accurate solutions of the scattering coefficients of E-plane junctions in rectangular waveguides. IEEE Trans. Microw. Theory Tech., **43** (1995), 2716–2718.

[6] Abdelmonem, A.; Yao, H.-W.; Zaki, K.A.: Slit coupled E-plane rectangular T-junctions using single port mode matching technique. IEEE Trans. Microw. Theory Tech., **42** (1994), 903–907.

[7] Blas, A.A.S.; Mira, F.; Boria, V.E.; Gimeno, B.; Bressan, M.; Arcioni, P.: On the fast and rigorous analysis of compensated waveguide junctions using off-centered partial-height metallic posts. IEEE Trans. Microw. Theory Tech., **55** (2007), 168–175.

[8] Wu, K.-L.; Wang, H.A.: A rigorous modal analysis of H-plane waveguide T-junction loaded with a partial-height post for wide-band applications. IEEE Trans. Microw. Theory Tech., **49** (2001), 893–901.

[9] Berdnik, S.L.; Katrich, V.A.; Nesterenko, M.V.; Penkin, Yu.M.: E-plane T-junction of rectangular waveguides with vibrator-slot coupling between arms. Telecomm. Radio Eng., **74** (2015), 1225–1240.

[10] Nesterenko, M.V.; Katrich, V.A.; Penkin, Yu.M.; Berdnik, S.L.: Analytical and Hybrid Methods in Theory of Slot-Hole Coupling of Electrodynamic Volumes, Springer Science+Business Media, New York, 2008.

[11] Nesterenko, M.V.; Katrich, V.A.; Penkin, Yu.M.; Dakhov, V.M.; Berdnik, S.L.: Thin Impedance Vibrators. Theory and Applications, Springer Science+Business Media, New York, 2011.

[12] Berdnik, S.L.; Katrich, V.A.; Nesterenko, M.V.; Penkin, Yu.M.; Penkin, D. Yu.: Radiation and scattering of electromagnetic waves by a multi-element vibrator-slot structure in a rectangular waveguide. IEEE Trans. Antennas Propag., **63** (2015), 4256–4259.

Sergey L. Berdnik received the degree (similar to M.S.) in Radiophysics and Electronics from V. N. Karazin Kharkiv National University, Kharkiv, Ukraine in 2000, and received his Ph.D. degree in 2010. From 2000 he has been a research worker and Assistant Professor with the Department of Radiophysics, V. N. Karazin Kharkiv National University. He is currently an Associate Professor, also part-time Senior Researcher. His research interests include electromagnetic

theory, diffraction's problems in applied electrodynamics, theory of waveguide-slot coupling elements and antennas array, theory of thin impedance vibrators and their arrays.

Victor A. Katrich was born in Kharkiv, Ukrainian SSR, on September 18, 1944. He received the degree (similar to M.S.) in Radiophysics and Electronics from M. Gorky Kharkiv State University, Kharkov, Ukraine in 1968, and the Ph.D. degree in 1981. Since 1968 he has been with the M. Gorky Kharkiv State University (now V. N. Karazin Kharkiv National University). Since 1981 he has been Senior Researcher at the Department of Radiophysics. From 2005 until now he is Full Professor, also part-time Principle Scientist. His research interests include electromagnetic theory, diffraction's problems in applied electrodynamics, theory of the waveguide-slot coupling elements, theory of radiation of the arbitrary length slots and curvilinear slots cut in walls of the single-mode and poly-modal waveguides.

Mikhail V. Nesterenko was born in Tallinn, Estonian SSR, on February 3, 1957. He received the degree (similar to M.S.) in Radiophysics and Electronics from M. Gorky Kharkiv State University, Kharkov, Ukraine in 1979, and the Ph.D. degree in 1989. Since 1979 he has been with the M. Gorky Kharkiv State University (now V. N. Karazin Kharkiv National University). Since 1989 he has been Senior Researcher at the Department of Radiophysics. From 2012 until now he is Doctor of Science and the Principle Scientist. His research interests include electromagnetic theory, diffraction's problems in applied electrodynamics, theory of thin impedance vibrators and their arrays, theory of waveguide-slot coupling elements.

Yuriy M. Penkin was born in Kharkiv, Ukrainian SSR, on July 29, 1960. He received the degree (similar to M.S.) in Radiophysics and Electronics from M. Gorky Kharkiv State University, Kharkiv, Ukraine in 1982, and the Ph.D. degree in 1988. Since 1982 he has been with the M. Gorky Kharkiv State University (now V. N. Karazin Kharkiv National University). Since 1988 he has been Senior Researcher at the Department of Radiophysics. From 2002 until now he is Full Professor, also part-time Senior Researcher. His research interests include electromagnetic theory, diffraction's problems in applied electrodynamics, theory of the waveguide-slot coupling elements and theory of the excitation of electromagnetic waves in volumes with curvilinear coordinate boundaries.